



THE UNIVERSITY *of* EDINBURGH

## Edinburgh Research Explorer

# MR elastography measurement of the effect of passive warmup prior to eccentric exercise on thigh muscle mechanical properties

### Citation for published version:

Kennedy, P, Macgregor, LJ, Barnhill, E, Johnson, CL, Perrins, M, Hunter, A, Brown, C, Van Beek, EJR & Roberts, N 2017, 'MR elastography measurement of the effect of passive warmup prior to eccentric exercise on thigh muscle mechanical properties', *Journal of Magnetic Resonance Imaging*, vol. 46, no. 4, pp. 1115-1127. <https://doi.org/10.1002/jmri.25642>

### Digital Object Identifier (DOI):

[10.1002/jmri.25642](https://doi.org/10.1002/jmri.25642)

### Link:

[Link to publication record in Edinburgh Research Explorer](#)

### Document Version:

Publisher's PDF, also known as Version of record

### Published In:

Journal of Magnetic Resonance Imaging

### Publisher Rights Statement:

This is an open access article under the terms of the Creative Commons Attribution-NonCommercial License, which permits use, distribution and reproduction in any medium, provided the original work is properly cited and is not used for commercial purposes.

### General rights

Copyright for the publications made accessible via the Edinburgh Research Explorer is retained by the author(s) and / or other copyright owners and it is a condition of accessing these publications that users recognise and abide by the legal requirements associated with these rights.

### Take down policy

The University of Edinburgh has made every reasonable effort to ensure that Edinburgh Research Explorer content complies with UK legislation. If you believe that the public display of this file breaches copyright please contact [openaccess@ed.ac.uk](mailto:openaccess@ed.ac.uk) providing details, and we will remove access to the work immediately and investigate your claim.



# MR Elastography Measurement of the Effect of Passive Warmup Prior to Eccentric Exercise on Thigh Muscle Mechanical Properties

Paul Kennedy, PhD,<sup>1,2</sup> Lewis J. Macgregor, PhD,<sup>3</sup> Eric Barnhill, PhD,<sup>4</sup> Curtis L. Johnson, PhD,<sup>5</sup> Michael Perrins, MSc,<sup>1</sup> Angus Hunter, PhD,<sup>3</sup> Colin Brown, BSc,<sup>6</sup> Edwin J.R. van Beek, MD,<sup>1</sup> and Neil Roberts, PhD<sup>1\*</sup>

**Purpose:** To investigate the effect of warmup by application of the thermal agent Deep Heat (DH) on muscle mechanical properties using magnetic resonance elastography (MRE) at 3T before and after exercise-induced muscle damage (EIMD).

**Materials and Methods:** Twenty male participants performed an individualized protocol designed to induce EIMD in the quadriceps. DH was applied to the thigh in 50% of the participants before exercise. MRE,  $T_2$ -weighted MRI, maximal voluntary contraction (MVC), creatine kinase (CK) concentration, and muscle soreness were measured before and after the protocol to assess EIMD effects. Five participants were excluded: four having not experienced EIMD and one due to incidental findings.

**Results:** Total workload performed during the EIMD protocol was greater in the DH group than the control group ( $P < 0.03$ ), despite no significant differences in baseline MVC ( $P = 0.23$ ). Shear stiffness  $|G^*|$  increased in the rectus femoris (RF) muscle in both groups ( $P < 0.03$ ); however, DH was not a significant between-group factor ( $P = 0.15$ ). MVC values returned to baseline faster in the DH group (5 days) than the control group (7 days). Participants who displayed hyperintensity on  $T_2$ -weighted images had a greater stiffness increase following damage than those without: RF; 0.61 kPa vs. 0.15 kPa,  $P < 0.006$ , vastus intermedius; 0.34 kPa vs. 0.03 kPa,  $P = 0.06$ .

**Conclusion:** EIMD produces increased muscle stiffness as measured by MRE, with the change in  $|G^*|$  significantly increased when  $T_2$  hyperintensity was present. DH did not affect CK concentration or soreness; however, DH participants produced greater workload during the EIMD protocol and exhibited accelerated MVC recovery.

**Level of Evidence:** 1.

J. MAGN. RESON. IMAGING 2016;00:000–000.

Exercise-induced muscle damage (EIMD) can occur following unaccustomed training, particularly in routines that incorporate eccentric exercise, and results in muscle pain, increased passive tension, reduced force output, and elevated blood markers such as creatine kinase (CK).<sup>1</sup> Eccentric movement exacerbates the response to unaccustomed exercise due to the forcible lengthening of myofibrils and associated disruption of sarcomeres, which is unique to eccentric contraction.<sup>1–3</sup> Histological examination of muscle samples following concentric

and eccentric contractions has previously revealed structural damage in only the eccentrically exercised muscles.<sup>4</sup> The severity of EIMD is reported to increase as a result of maximal eccentric contractions<sup>5</sup> and also with training duration.<sup>6</sup> EIMD not only occurs in untrained individuals, trained athletes are also susceptible.<sup>7–9</sup> Following EIMD, participants have been reported to experience increased intramuscular pressure in the affected muscle compartments,<sup>10</sup> which has been associated with increased passive tension<sup>11,12</sup> as well as often showing

View this article online at [wileyonlinelibrary.com](http://wileyonlinelibrary.com). DOI: 10.1002/jmri.25642

Received Oct 3, 2016, Accepted for publication Jan 6, 2017.

\*Address reprint requests to: N.R., Clinical Research Imaging Centre (CRIC), University of Edinburgh, EH16 4TJ UK. E-mail: [neil.roberts@ed.ac.uk](mailto:neil.roberts@ed.ac.uk)

This is an open access article under the terms of the Creative Commons Attribution-NonCommercial License, which permits use, distribution and reproduction in any medium, provided the original work is properly cited and is not used for commercial purposes.

From the <sup>1</sup>Clinical Research Imaging Centre (CRIC), Queen's Medical Research Institute, University of Edinburgh, Edinburgh, UK; <sup>2</sup>Translational and Molecular Imaging Institute (TMII), Icahn School of Medicine at Mount Sinai, New York, USA; <sup>3</sup>Health and Exercise Research Group, School of Sport, University of Stirling, UK; <sup>4</sup>Department of Radiological Science, Charité-Universitätsmedizin, Berlin, Germany; <sup>5</sup>Department of Biomedical Engineering, University of Delaware, Newark, Delaware, USA; and <sup>6</sup>The Mentholatum Company Ltd, East Kilbride, Glasgow, UK

hyperintensity on  $T_2$ -weighted magnetic resonance imaging (MRI) images.<sup>13</sup> To minimize the effects of EIMD<sup>14,15</sup> and reduce the incidence of muscle injury,<sup>16–18</sup> dynamic and passive warmup routines are common practice among professional and amateur athletes (see Ref. 19 for review). Evidence to support the benefits of increasing muscle temperature has been previously reported; for example, superficial passive heating applied alongside a low-load static stretch has been shown to increase joint mobility compared to stretching alone.<sup>20,21</sup> Animal studies have also reported that the force required to damage muscle is increased when muscle temperature is raised.<sup>22–24</sup> Methods of passively increasing tissue temperature such as diathermy and ultrasound are often impractical to use. An alternative is to apply a thermal agent such as Deep Heat (DH) (The Mentholatum Company Ltd., East Kilbride, UK), which has been shown by thermography to produce an, at least, superficial warming effect.<sup>25</sup> DH has not been evaluated in treating the symptoms of EIMD; however, superficial warming has shown benefits in reducing muscle pain following EIMD.<sup>26</sup> DH also contains salicylates which are effective in acute pain relief.<sup>27</sup> In the present study we used MR elastography (MRE) to measure the stiffness of skeletal muscle affected by EIMD *in vivo* to investigate whether this provides imaging-based evidence that passive warmup prevents muscle injury.

MRE is a phase-contrast MRI technique<sup>28</sup> that images the passage of externally induced sound waves through tissues. Increases in muscle stiffness are detected as an increase in the wavelength of the sound waves, and so may be quantified. MRE provides a direct quantitative measure of muscle belly stiffness by measurement of the complex shear modulus. Direct measurement of the muscle belly stiffness removes contributions from sources other than the muscle group in question, e.g., synergists and antagonist muscle groups, skin, ligaments, tendons, and articular structures,<sup>29</sup> which may be a factor in other methodologies used to indirectly measure muscle stiffness such as range of motion analysis<sup>30</sup> and tensiomyography (TMG).<sup>31</sup> MRE has previously been applied to muscle by Dresner et al,<sup>32</sup> who showed that muscle stiffness increased with applied load, and Klatt et al,<sup>33</sup> who showed that muscle stiffness increases linearly with strength of contraction. Barnhill et al<sup>34</sup> studied the pattern of activation of individual muscles of the quadriceps during contraction of the thigh and Green et al<sup>35</sup> investigated the effect of repeated eccentric contraction produced by downhill walking in seven participants, which was reported to produce an ~20% increase in muscle stiffness, although complementary physiological or biochemical measurements of the extent of muscle damage were not obtained.

Several different mechanisms have been proposed for the increase in muscle stiffness due to unaccustomed exercise. Howell et al<sup>36</sup> suggested that an increase in muscle stiffness is directly due to contraction caused by release of  $Ca^{2+}$  ions from damaged muscle sarcomeres, but this mechanism has been

disputed.<sup>37</sup> An alternative suggestion is that increased stiffness may be due to an increase in extracellular fluid causing swelling.<sup>38</sup> However, this mechanism has also been disputed on the basis that an increase in stiffness can be detected immediately postexercise before swelling occurs.<sup>39</sup>

The goal of the present study was to investigate whether warmup by topical application of the thermal agent DH rub provides protection against EIMD produced via repeated extension of the lower leg against an opposing force. The opposing force overwhelms the participant's capacity to concentrically contract, and hence the movement becomes an eccentric contraction, i.e., muscle fibers are forcibly lengthened. Leg extension is an Open Kinetic Chain Exercise (OKCE) due to the free distal portion of the limb. This differentiates leg extension from a Closed Kinetic Chain Exercise (CKCE) such as a squat, where the distal portion of the limb is weight-bearing. The leg extension is expected to preferentially stress the rectus femoris (RF) muscle, which has been shown to both activate earlier than the other quadriceps muscles<sup>40</sup> and produce increased EMG activity<sup>41</sup> during OKCE compared to CKCE. Furthermore, the RF is a biarticular muscle that acts across the hip and knee joints. It has been reported that seated eccentric exercise (hip angle 90°), as used in this study, produces elevated EIMD effects in the RF when compared to prone eccentric exercise (hip angle 180°).<sup>42</sup> The RF length change between seated and prone position has been estimated at 19%.<sup>43</sup> We predicted that application of DH would result in 1) a smaller increase in muscle stiffness as measured by MRE; 2) less hyperintensity indicative of edema on  $T_2$ -weighted MR images; 3) less reduction in force output as measured by maximum voluntary contraction (MVC); 4) smaller increase in plasma concentration of the muscle damage marker CK; and 5) lower pain scores in comparison to a control group in whom a placebo cream was applied. A secondary aim was to investigate whether muscle stiffness is significantly increased in muscles displaying  $T_2$  hyperintensity.

## Materials and Methods

### Participants

The study was approved by the local National Health Service Research Ethics Committee (REC). Participants were excluded if they were >35 years of age, had an existing muscular injury or were currently taking nonsteroidal anti-inflammatory drugs (NSAIDs). Twenty healthy male volunteer participants (mean age 24.1 years  $\pm$  4.3 years) who engaged in sporting activities at least three times a week were recruited and provided fully informed written consent of their willingness to participate. Participants were instructed to engage in no strenuous activity 3 days prior to participating in the study.

### EIMD Protocol

Two days prior to the first measurement session, participants completed a familiarization session at the School of Sport, University of Stirling. The familiarization session was designed to limit the impact of a learning effect on subsequent measurements. Maximum

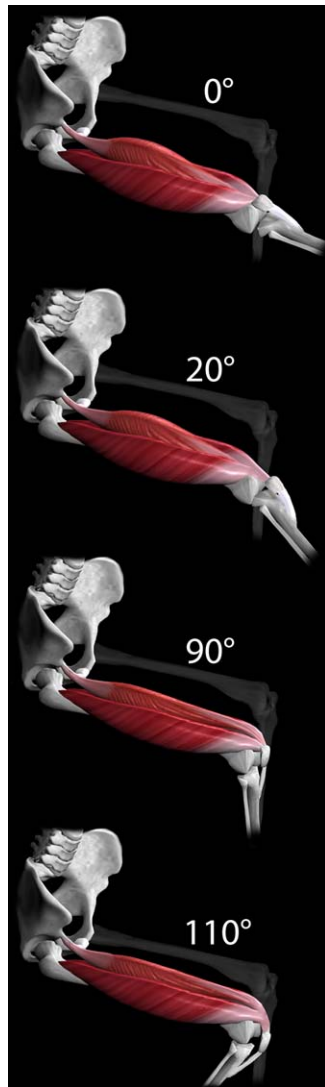


**FIGURE 1:** Illustration of the biarticular structure of the RF muscle group. Knee reference angles described during the EIMD protocol are also annotated. Adapted with permission from [muscleandmotion.net](http://muscleandmotion.net)

voluntary contraction (MVC) measurements and the EIMD protocol were performed using an isokinetic dynamometer (System 3, Biodex Medical Systems, New York, NY). During the familiarization session the required movements and measurements were demonstrated and practiced on this system but without any strenuous exercise.

The participant was seated in the dynamometer and straps were placed across the chest, hips, and nondominant leg. The dominant leg was affixed to the dynamometer arm via Velcro straps placed above the ankle. The knee angle was considered  $0^\circ$  when the participant fully extended their leg in front of them, describing a  $0^\circ$  angle to the horizontal. When the knee was bent at right angles the knee angle was considered  $90^\circ$  (Fig. 1). MVC measurements were performed isometrically at a knee angle of  $60^\circ$ , which has been previously reported to fall within the optimum knee angle for peak isometric force production.<sup>44</sup> The participant was first instructed to warmup by performing six isometric contractions, each lasting 5 seconds with subjectively increasing force, and with a 10-second rest between contractions. For MVC

measurements an audio stimulus was played, upon hearing which the participant contracted maximally for 5 seconds. This process was repeated three times with a random interval between stimuli to prevent the participants anticipating the movement. Fatigue had no impact over the three trials with an average force reduction between Trials 1 and 3 of 0.2%. The audio stimulus and force data were recorded using Acknowledge software (BIOPAC Systems, Santa Barbara, CA) and the peak MVC force over the three trials was calculated.

Following baseline MVC measurement, participants were randomly assigned to one of two groups: those in the DH group applied 5g of DH rub to the surface of the thigh above the quadriceps muscles of the dominant leg, whereas participants in the control group applied a placebo moisturizing cream to the same area. Participants then rested for 25 minutes in a relaxed seated position before cycling on an ergometer (Lode Excalibur Sport V2 electrically braked cycle ergometer, Lode, Groningen, Netherlands) for 5 minutes at 70 rpm and  $\sim 50$ W to ensure some level of warmup was undertaken by all participants prior to the EIMD protocol.

The EIMD protocol was split into 12 sets, each completed once the participant reached an individually calculated workload. The workload was based on the peak eccentric and concentric forces generated by a participant during a repetition, which consisted of an eccentric phase and concentric phase over a  $90^\circ$  range of motion—from a knee angle of  $20^\circ$  to  $110^\circ$ . During each repetition the participant continuously contracted the quadriceps, i.e., attempted to extend the leg. In order to induce eccentric contraction, the Biodex dynamometer forcibly flexed the knee when an extension force  $>50$  Nm was detected. This flexion forcibly lengthened the muscle fibers, causing eccentric damage. The eccentric phase occurred from the starting point at a knee angle of  $20^\circ$  to the end of the range of motion at  $110^\circ$ . Upon reaching the  $110^\circ$  point, the Biodex ceased the forced knee flexion and the participant returned the dynamometer arm to the  $20^\circ$  starting point using voluntary concentric contraction. Completion of the eccentric phase ( $20^\circ \rightarrow 110^\circ$  knee angle) and concentric phase (returning from  $110^\circ$  to  $20^\circ$  knee angle) was considered one repetition.

In order to calculate a workload, each participant performed three repetitions of the EIMD protocol movement, each separated by 2 minutes. The peak eccentric and concentric forces were determined and the sum was multiplied by an estimated number of total reps to complete each set (taken as 10). This figure was then multiplied by 1.2 to ensure the muscles were maximally worked. Once the workload was reached the set was completed and the participant had a 2-minute rest before engaging in the subsequent set.

### **MRI Protocol**

MRI data were acquired using a 3T MRI system (Verio, Siemens Medical Systems, Erlangen, Germany). Investigations were performed at baseline ( $<24$  hours before EIMD protocol) and again 48 hours after the EIMD protocol.

For MRE experiments, mechanical excitation was introduced to the thigh via a plastic actuator ring connected to the vibration source via a carbon fiber rod. The actuator was designed at the MRE Research Laboratory, Charité-Universitätsmedizin Berlin, Germany<sup>33</sup> and was firmly secured around the leg using Velcro straps to ensure sufficient wave transmission. A cod liver oil capsule

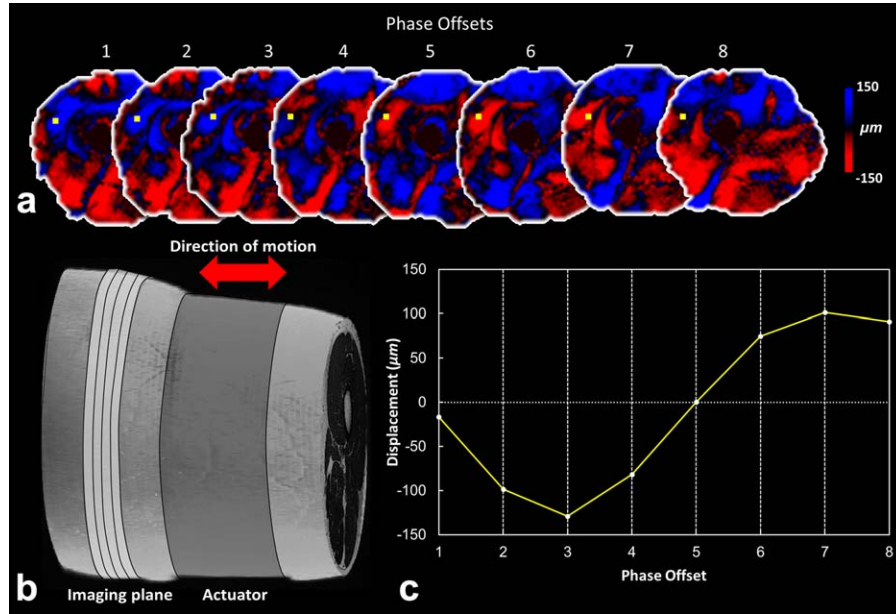


**FIGURE 2:** Wave images from a single image slice illustrating the wave propagation over eight phase offsets (a). A 3D volume rendering (b) of a  $T_2$  acquisition shows the compression from the ring actuator which transmits externally generated waves into the tissue. The image plane is also labeled. In (c) the evolution of wave propagation across the eight phase offsets is depicted by plotting the displacement at a point (yellow marker in (a)) during each offset.

was placed on the actuator to facilitate image plane positioning, which was prescribed 2 cm above the proximal actuator edge to avoid potential effects of compression of the muscle by the actuator ring.<sup>45</sup> The distance from the distal end of the actuator ring to the proximal surface of the patella was measured to ensure identical image plane placement during the follow-up visit. A 32-channel flexible array coil was placed around the thigh to record the MR signals. An example of wave propagation and actuator and imaging plane placement are shown in Fig. 2.

Prior to the carbon fiber rod being connected between the loudspeaker and the actuator, a localizer scan was performed followed by a high-resolution turbo spin echo (TSE) sequence to provide transverse  $T_2$ -weighted images through the thigh for the same sections as would subsequently be studied using MRE. The acquisition parameters for the TSE images were TE 96 msec, TR 4430 msec, slice thickness 3 mm, bandwidth 407 Hz per pixel, field of view (FOV) of  $200 \times 200$  mm, and image matrix of  $512 \times 512$  giving a final voxel size of  $0.4 \times 0.4 \times 3$  mm<sup>3</sup>. A total of 48 contiguous slices were acquired with two averages to improve signal-to-noise ratio (SNR).

MRE data were acquired using a spin-echo echo planar imaging (EPI) MRE sequence<sup>33,34</sup> to produce 3D displacement fields for mechanical vibration frequencies of 25 Hz, 37.5 Hz, 50 Hz, and 62.5 Hz with motion encoding applied in turn in phase-encoding, slice-select, and readout directions. The acquisition parameters were TE 54 msec, TR 1600 msec, 1 motion encoding gradient (MEG) cycle at 50 Hz, and a bandwidth of 1560 Hz per pixel. A total of five 2-mm-thick contiguous slices were imaged with an in-plane FOV of  $224 \times 224$  mm and image matrix of  $112 \times 112$ ; voxel size was  $2 \times 2 \times 2$  mm<sup>3</sup>, eight phase offsets were obtained at each actuation frequency and two averages were used to increase SNR. All acquired images were reviewed for incidental findings by a radiologist (E.J.V.B.) with 18 years of experience.

### Image Analysis

MRE data analysis was performed using phase unwrapping<sup>46</sup> and inversion software called ESP<sup>47</sup> running in MatLab (MathWorks, Natick, MA) with several simplifying assumptions including viscoelasticity, local homogeneity, and mechanical isotropy. These assumptions allow calculation of the complex modulus  $G^*$  from the temporally Fourier-transformed 3D displacement field  $U$  using the Helmholtz-type equation<sup>48</sup>:

$$G^* = -\rho\omega^2 \frac{U}{\Delta U} \quad (1)$$

where  $\rho$  is tissue density ( $1050 \text{ kg m}^{-3}$ ),  $\omega$  is the angular frequency of the mechanical oscillation, and  $\Delta$  denotes the Laplace operator. The complex modulus  $G^*$  is defined as the sum of the real storage modulus  $G'$ , a measure of tissue elasticity, and the imaginary loss modulus  $G''$ , a measure of tissue viscosity. Further details of the inversion scheme can be found in Ref. 47. The viscoelastic parameters reported are the magnitude of the complex modulus  $|G^*|$  and its phase angle  $\varphi$  defined as the ratio of  $G'$  and  $G''$  and considered to be a measure of tissue viscosity.<sup>47</sup>

MRE image quality was assessed by applying the octahedral shear strain SNR (OSS-SNR) method,<sup>49</sup> which has been frequently utilized in MRE studies.<sup>50,51</sup> An OSS-SNR threshold of 3 is considered to yield stable stiffness results.

Regions of interest (ROIs) corresponding to the rectus femoris (RF), vastus intermedius (VI), vastus medialis (VM), and vastus lateralis (VL), as well as the entire quadriceps (i.e., RF, VI, VM, and VL combined) and entire hamstrings were drawn separately on the MRE magnitude images using ImageJ.<sup>52</sup> Care was taken to ensure muscle fascia was not included in the ROIs. Values of  $|G^*|$  and  $\varphi$  were extracted for the above ROIs.

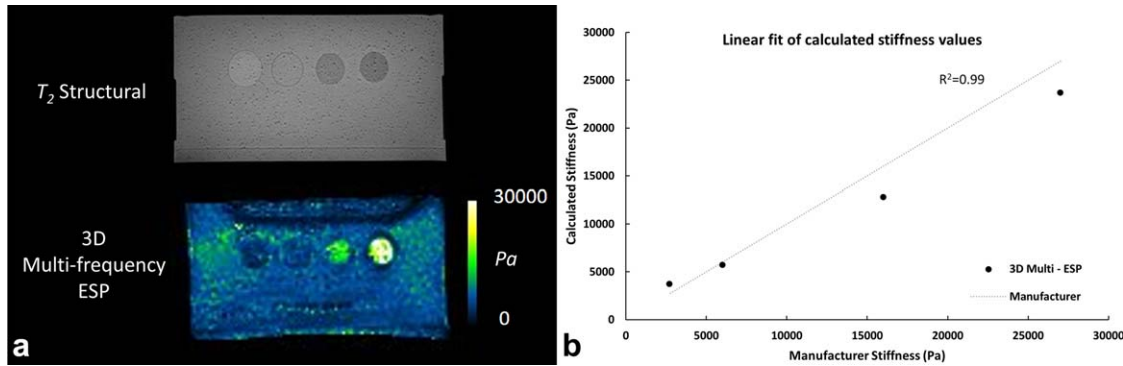


FIGURE 3: (a)  $T_2$ -weighted image and elastogram of the CIRS 049 test object and (b) plot of stiffness values measured for the four inclusions plotted against values given by the test object manufacturer.

### Baseline and Postdamage Measurement of EIMD Symptoms

A number of additional measurements were obtained to enable assessment of the compliance of participants in performing the EIMD protocol, the severity of damage produced, and recovery. The following measures were recorded at the School of Sport, University of Stirling at baseline, and 2, 5, 7 and 9 days after the EIMD protocol.

#### Maximum Voluntary Contraction (MVC) Recovery

Loss of muscle force as measured by reduction in MVC is frequently reported in studies of EIMD.<sup>53,54</sup> MVC of the dominant leg was therefore recorded using the same Biodex Isokinetic Dynamometer, which had been used for delivering the EIMD protocol. A force loss of 10% was subsequently applied to identify participants who had developed EIMD.<sup>25</sup>

#### Plasma Creatine Kinase (CK) Analysis

On each visit, prior to which participants had fasted overnight, 10 mL of venous blood was collected in an EDTA-containing vacuum tube from the participant's antecubital fossa. The sample was then centrifuged at 3500 rpm for 15 minutes at 4°C, after which the separated plasma was aliquoted evenly into Eppendorf tubes and stored at -80°C. Enzymatic analysis of plasma CK concentration was performed in duplicate at each timepoint using a semiautomated analyzer (iLab Aries, Instrumentation Laboratory, Bedford, MA).

#### Subjective Pain Rating of Pressure Stimulus

In order to obtain a subjective rating of the sensitivity of the participant to a pressure stimulus, a custom-built spring-loaded algometer was used to apply 1 kg per cm force at the level of the head of the RF muscle while the leg was in flexed (i.e., sitting in the Biodex system with leg at 90° knee angle) or extended (i.e., sitting and with the leg lifted to 0° knee angle) positions. During pressure application the participant was instructed to rate their perceived muscle soreness using a 200 mm visual analog scale (VAS). Participants marked the appropriate point along the continuum from a rating of "No Pain" to "Most Pain Imaginable." The distance between the "No Pain" rating and the participant's mark was measured to quantify muscle soreness.

#### MRE Protocol Quality Assurance

The CIRS 049 test object (Computerized Imaging Reference Systems (CIRS), Norfolk, VA) which has been previously used for

quality assurance in MRE,<sup>55,56</sup> and in ultrasound elastography,<sup>57,58</sup> was studied using the same MRE sequence and ESP analysis pipeline as was used for the in vivo investigations. The test object was constructed from a synthetic elastic substance known as Zerdine and contained eight spherical inserts (four with a diameter of 20 mm and four with a diameter of 10 mm) of increasing stiffness measured by the manufacturer via quasistatic compression testing. The imaging volume was prescribed to include all four 20 mm inclusions and the test object was vibrated at 25, 37.5, 50, and 62.5 Hz using a paddle actuator. ROIs were traced inside the boundaries of the four inserts using ImageJ and computed values of  $|G^*|$  were compared to manufacturer reported values. Mean stiffness was calculated over the five image slices. A total of eight acquisitions were performed with the test object removed and repositioned in the MR system for each acquisition in order to assess reproducibility.

#### Statistical Testing

Statistical significance of within-participant effects over time of MRE, MVC, CK, and pain measurements were assessed using a two-tailed Wilcoxon signed-rank test. Differences between DH and control groups were tested for significance using unpaired Mann-Whitney  $U$ -tests. Cohen's  $d$  effect size values were calculated with 0.2, 0.5, and 0.8 considered as small, moderate, and large effects.<sup>59</sup> Relationship between measurement variables was assessed using Pearson's correlation. Coefficient of variation was calculated for the phantom acquisitions. Fisher's exact test was used to compare the incidence of  $T_2$  hyperintensity in the DH and control group. All statistical tests were performed using SPSS Statistics (v. 20, IBM, Armonk, NY). A  $P$ -value <0.05 was considered significant.

## Results

### MRE Phantom Measurements

The  $T_2$ -weighted images and elastograms shown in Fig. 3a confirm that the inclusions could be readily detected in the CIRS 049 test object and in Fig. 3b the measured stiffness of each inclusion is plotted against corresponding values provided by the manufacturer (Table 1). The linear relationship between measured and manufacturer values was statistically significant ( $r = 0.99$ ,  $P < 0.005$ ). The coefficient of variation (CV) was less than 5% over the eight repeated investigations.

**TABLE 1. Measured and Manufacturer Provided Values for Stiffness of Inclusions in CIRS 049 Test Object (Pa)**

Testing Method	Target 1	Target 2	Target 3	Target 4
Quasi-static (manufacturer)	2700	6000	16000	27000
3D Multi-frequency MRE	3731 ± 189	5722 ± 198	12827 ± 291	23713 ± 241

### Compliance and Performance on EIMD Protocol

Details of the performance of individual participants in completing the EIMD protocol are presented in Table 2. In order to ensure that all participants included in the analysis had experienced EIMD a threshold of >10% MVC reduction between baseline and the first postexercise measurement was applied (Fig. 4). This threshold led to the exclusion of four participants from subsequent analyses. These participants were found to have completed the EIMD protocol with consistent repetitions per set, suggesting that the workload target that had been set for these participants was not sufficiently taxing. Three of the four participants (#10, #18 and #20) were from the DH group and one (#11) was from the control group. In addition, a control group participant (#13) was removed due to the incidental finding of an area of calcification being identified in the RF muscle during review by a radiologist. Thus, 15 participants remained, seven in the DH group and eight in the control group. There was no significant difference in mean baseline MVC between the final DH group and the control group ( $P = 0.23$ ). However, total work performed by the DH group was significantly greater than by the control group ( $P < 0.03$ ).

### Effect of DH on Physiological and Biochemical Measurements

Both the DH group and control group showed a significant increase in CK concentration ( $P < 0.03$ ), increase in pain score ( $P < 0.05$ ), and decrease in MVC ( $P < 0.02$ ) after 48 hours compared to baseline (Fig. 5). The magnitude of the effect was generally greater in the DH group than the control group for MVC (mean decrease 105 Nm, Cohen's  $d$  1.67 vs. 62 Nm, 2.27) and CK (mean increase 633 IU/l, Cohen's  $d$  0.89 vs. 514 IU/l, 1.19) but the increase in subjective pain was reduced in the DH group in both extension (mean increase 3.7, Cohen's  $d$  0.95 vs. 3.75, 0.67) and flexion (mean increase 1.85, Cohen's  $d$  0.96 vs. 2.79, 0.64). However, Mann-Whitney  $U$ -tests revealed that 48 hours postexercise there were no significant differences between the groups for any of the physiological or biochemical measures (MVC  $P = 0.88$ , pain  $P > 0.85$ , CK  $P = 0.90$ ). Pain measurements in flexion and extension 48 hours after the protocol were highly correlated in both DH and control groups ( $r = 0.978$ ,  $P < 0.001$  and  $r = 0.982$ ,  $P < 0.001$ , respectively).

Five days after the EIMD protocol MVC measurements for the DH group were not significantly different than baseline ( $P > 0.24$ , Cohen's  $d$  0.61). However, the control group was still producing significantly lower force at this timepoint ( $P < 0.02$ , Cohen's  $d$  1.89), indicating faster recovery in the DH group. CK concentration was significantly increased in both groups over the entire study period ( $P < 0.05$ ). Pain measurements in extension and flexion were not significantly different from baseline in either group after 5 ( $P > 0.25$ ), 7 ( $P > 0.21$ ), and 9 ( $P > 0.39$ ) days post-EIMD protocol. No long-term adverse effects resulted from completion of the EIMD protocol.

### Effect of DH on Stiffness of the Damaged Muscle

Example images of  $|G^*|$  and  $\phi$  for four of the participants are shown in Fig. 6. Mean OSS-SNR was >3 in all but three participants. Of these three cases OSS-SNR was <3 in the hamstrings (2/3 cases) and the VM (1/3 cases). Two participants, one with OSS-SNR <3 in the hamstrings and one with OSS-SNR <3 in the VM were excluded from analysis having not experienced an MVC reduction of >10%. In the other case, with OSS-SNR <3 in the hamstrings, the hamstrings measurement from that participant was excluded. Analysis of the MRE data (Table 4) revealed a significant increase in  $|G^*|$  in the RF muscle in both the DH ( $P < 0.02$ , Cohen's  $d$  1.29) and control groups ( $P < 0.03$ , Cohen's  $d$  0.81) 48 hours after the EIMD protocol (Fig. 7). In addition, there was a trend whereby the VI muscle group also showed an increase in  $|G^*|$  in the DH Group ( $P = 0.06$ , Cohen's  $d$  0.86). These findings are consistent with the CK and MVC changes in indicating greater damage in the DH group, although the differences between groups were not significant ( $P = 0.09$ ). Analysis of the second MRE parameter,  $\phi$ , for the RF and VI muscles revealed there to be no significant changes in either the DH or control group following the EIMD protocol. However, in the DH group  $\phi$  was significantly increased in both the VM muscle group ( $P < 0.03$ ) and over the entire quadriceps ROI ( $P < 0.02$ ) following the EIMD protocol, with no corresponding effect observed in the control group.

### Effect of DH on $T_2$ -weighted Images

Inspection of the  $T_2$ -weighted images revealed that hyperintense signal was localized to the RF (6/15 participants [40%]; three in the DH group and three in the control group) with diffuse hyperintensity also present in the VI

TABLE 2. EIMD Protocol Performance Results and MVC Data for 20 Participants

Subject	DH	$T_2$ RF	$T_2$ VI	MVC (Nm)	MVC change (%)	Workload (J)	Total Reps
1	No	No	No	316	-20	3871	156
2	Yes	Yes	Yes	269	-55	3778	179
3	No	No	No	197	-32	3227	224
4	Yes	Yes	Yes	355	-51	5972	291
5	No	Yes	No	260	-18	4538	349
6	No	Yes	Yes	213	-55	4200	273
7	Yes	No	Yes	406	-44	4789	152
8	Yes	Yes	No	220	-34	5400	285
9	No	Yes	No	375	-14	5193	365
10	Yes	No	No	213	-4	3121	146
11	No	No	No	252	9	3722	147
12	Yes	No	Yes	254	-18	5209	312
13	No	Yes	Yes	266	-54	5055	326
14	Yes	No	No	227	-31	6007	353
15	No	No	No	167	-19	3245	124
16	Yes	No	No	276	-12	5901	216
17	No	No	No	255	-34	5773	296
18	Yes	No	No	219	1	3932	170
19	No	No	No	188	-21	3619	177
20	Yes	No	No	222	3	3704	156

Participants highlighted with gray cells were excluded from the analysis (#10, #11, #13, #18, and #20). Participant #13 was removed due to the presence of an incidental finding.

(5/15 participants [33%]; four in the DH group and one in the control group) muscle groups. Fisher's exact test revealed that the occurrence of hyperintensity in RF and VI muscles was not significantly related to the application of DH ( $P < 0.6$  and  $P > 0.1$ , respectively).

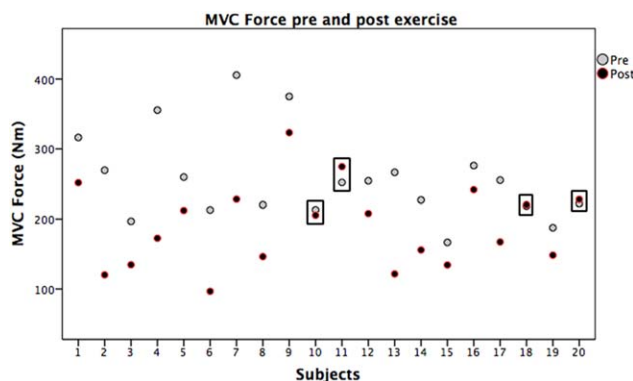


FIGURE 4: MVC force data for all participants at baseline and 2 days after EIMD protocol. The rectangles highlight the four participants in whom the reduction in MVC was <10%.

Participants displaying RF and VI  $T_2$  hyperintensity had significantly increased  $|G^*|$  compared to baseline after 48 hours ( $1.16 \pm 0.21$  kPa  $\rightarrow$   $1.77 \pm 0.34$  kPa,  $P < 0.03$  and  $1.29 \pm 0.05$  kPa  $\rightarrow$   $1.63 \pm 0.22$  kPa,  $P < 0.05$ , respectively). Participants without hyperintense  $T_2$  signal also showed a significant increase in RF stiffness after 48 hours ( $1.31 \pm 0.33$  kPa  $\rightarrow$   $1.46 \pm 0.39$  kPa,  $P < 0.02$ ); however, VI stiffness was not significantly different ( $1.33 \pm 0.23$  kPa  $\rightarrow$   $1.36 \pm 0.31$  kPa,  $P > 0.5$ ).

Analysis of the mean increase in  $|G^*|$  of the RF and VI between participants who displayed hyperintensity on  $T_2$ -weighted images and those who did not showed that the mean increase in  $|G^*|$  of the RF was significantly higher in participants with  $T_2$  hyperintensity following damage compared to participants without  $T_2$  hyperintensity ( $0.61 \pm 0.31$  kPa vs.  $0.15 \pm 0.17$  kPa,  $P < 0.006$ ). A similar trend was observed in the VI muscle group, with participants with  $T_2$  hyperintensity having a greater mean  $|G^*|$  increase following damage, although it did not reach significance ( $0.34 \pm 0.26$  kPa vs.  $0.03 \pm 0.36$  kPa,  $P = 0.06$ ).



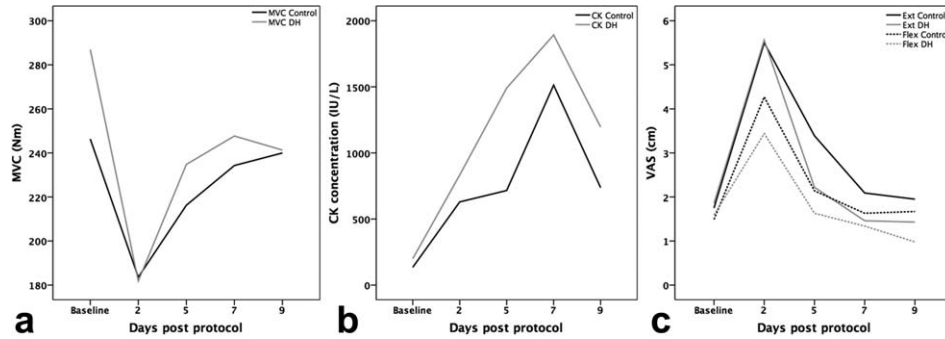


FIGURE 5: Time course of (a) MVC, (b) CK concentration, and (c) pain at baseline and during recovery from the EIMD protocol. Error bars are omitted for clarity. SD values are presented in Table 3.

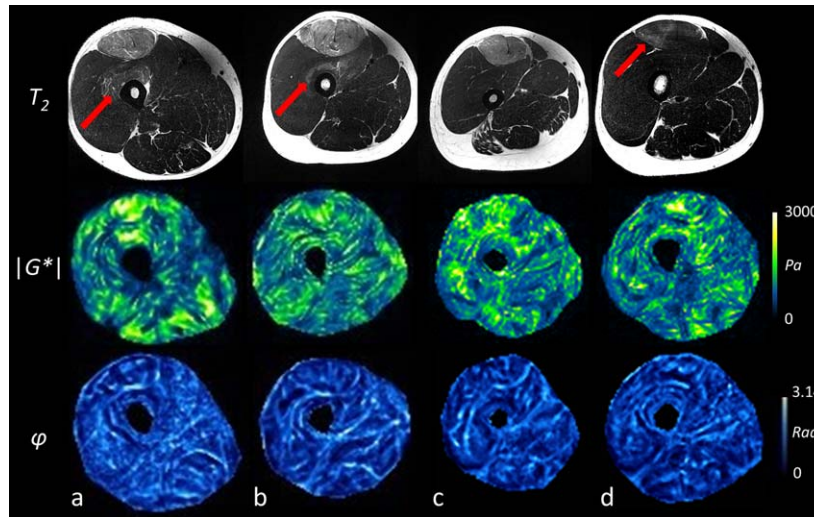


FIGURE 6: T<sub>2</sub>-weighted images and maps of  $|G^*|$  and  $\varphi$  for four participants. Hyperintensity on T<sub>2</sub>-weighted images suggests edema is present in the RF (a–d) and VI muscle groups (a,b). Less severe hyperintensity is denoted by red arrows.

**Discussion**

The CIRS 049 phantom had been previously used to verify MRE measurements.<sup>55,56</sup> In both cases different inversion approaches to the ones used here (i.e., finite element modeling) were applied; however, the recovered stiffness values were found to be lower than values reported by the manufacturer

for the stiffest target and higher for the softest target. This was reflected in the results generated in this study also. The discrepancy between the calculated stiffness and the manufacturer reported values could be due to several factors. For example, the manufacturer may have performed the measurements at a lower frequency. Alternatively, temperature variations could

TABLE 3. Mean Values of MVC, Pain Score, and CK Concentration Over the Study Period for the Seven Participants in the DH Group and the Eight Participants in the Control Group

Measurement	MVC (Nm)		Pain (VAS cm)				CK (IU/L)	
	Control	DH	Control Ext	Control Flex	DH Ext	DH Flex	Control	DH
Baseline	246.3 ± 66.5	286.9 ± 63.6	1.8 ± 1.2	1.5 ± 0.8	1.9 ± 1.1	1.6 ± 0.6	135 ± 58	199 ± 129
48 hours	183.6 ± 69.7	181.9 ± 41.8	5.5 ± 5.5	4.3 ± 4.3	5.6 ± 3.3	3.4 ± 1.8	629 ± 381	833 ± 691
5 days	216.2 ± 65.8	234.8 ± 32.2	3.4 ± 2.6	2.1 ± 0.8	2.2 ± 0.8	1.6 ± 0.7	716 ± 805	1491 ± 1457
7 days	234.3 ± 71.2	247.7 ± 36.1	2.1 ± 1.4	1.6 ± 1.0	1.5 ± 1.0	1.3 ± 0.9	1513 ± 1246	1893 ± 1024
9 days	240.0 ± 75.4	241.3 ± 28.4	2.0 ± 1.5	1.7 ± 1.6	1.4 ± 1.6	1.0 ± 0.6	737 ± 613	1196 ± 985

**TABLE 4. Mean Values of the Magnitude of the Complex Shear Modulus ( $|G^*| \pm SD$ ) and phase angle ( $\phi$ ) are Presented for the Rectus Femoris (RF), Vastus Intermedius (VI), Vastus Medialis (VM), Vastus Lateralis (VL), Quadriceps (Quad), and Hamstrings (Ham) in the DH and Control Groups at Baseline and After the EIMD protocol**

Muscle Group	Control Group						Deep Heat Group					
	$ G^* $ (kPa)			$\phi$ (rad)			$ G^* $ (kPa)			$\phi$ (rad)		
	Pre Damage	Post Damage	Muscle Group	Pre Damage	Post Damage	Muscle Group	Pre Damage	Post Damage	Muscle Group	Pre Damage	Post Damage	Muscle Group
VM	1.15 ± 0.18	1.12 ± 0.09	VM	0.76 ± 0.07	0.86 ± 0.10*	VM	1.19 ± 0.20	1.17 ± 0.22	VM	0.84 ± 0.07	0.77 ± 0.09*	VM
RF	1.26 ± 0.37	1.48 ± 0.36*	RF	0.79 ± 0.08	0.85 ± 0.08	RF	1.23 ± 0.12	1.69 ± 0.37**	RF	0.80 ± 0.08	0.77 ± 0.10*	RF
VI	1.38 ± 0.20	1.35 ± 0.29	VI	0.85 ± 0.08	0.89 ± 0.08	VI	1.24 ± 0.13	1.50 ± 0.29*	VI	0.82 ± 0.13	0.83 ± 0.08	VI
VL	1.19 ± 0.16	1.23 ± 0.11	VL	0.71 ± 0.06	0.79 ± 0.09	VL	1.21 ± 0.14	1.16 ± 0.04	VL	0.74 ± 0.07	0.71 ± 0.05	VL
Quad	1.15 ± 0.12	1.15 ± 0.10	Quad	0.80 ± 0.02	0.85 ± 0.05	Quad	1.17 ± 0.09	1.22 ± 0.10	Quad	0.82 ± 0.05	0.80 ± 0.04*	Quad
Ham	1.04 ± 0.12	1.05 ± 0.09	Ham	0.82 ± 0.05	0.86 ± 0.06	Ham	1.03 ± 0.07	1.00 ± 0.05	Ham	0.82 ± 0.05	0.81 ± 0.03	Ham

Also presented are the significant results from Mann-Whitney  $U$ -tests assessing the significance of changes in  $|G^*|$  and  $\phi$  (\* $P < 0.03$ ).

also be a cause, with the investigations in the present study being performed at room temperature and the testing by the manufacturer likely to have been performed under controlled conditions of temperature and humidity.

An important result of the present study is the identification of the main sites of muscle damage produced by an EIMD protocol of this type. Previous nonimaging-based studies have focused on the study of biopsies obtained from the VL muscle alone, likely due to the accessibility for biopsy.<sup>60–62</sup> Future studies, whether imaging-based or not, need to take into account the fact that the principal site of damage produced using this EIMD protocol is likely to be the RF and VI, and not the VL.

Analysis of the MRE data revealed that the magnitude of shear stiffness,  $|G^*|$ , was significantly increased in the RF muscle in both groups.  $|G^*|$  was also increased in the VI muscle in the DH group, although the difference compared to the control group was not significant. Hyperintensity on  $T_2$ -weighted images was more often present in the DH group than the control group (71% vs. 50%), although the difference was not significant. Analysis also showed that  $|G^*|$  of the RF and VI was significantly increased in the present of  $T_2$  hyperintensity. This indicates the presence of edema and potentially highlights an association between edema and increased stiffness measured by MRE.

The present study is the first in which MRE has been applied to investigate EIMD of the quadriceps muscles after eccentric exercise. A previous study<sup>35</sup> focused on the lower leg muscles, namely, the medial gastrocnemius and soleus and reported a significant 21% increase in storage modulus ( $G'$ ) of the medial gastrocnemius 48 hours postexercise. The soleus muscle group showed no significant increase after 48 hours but a 9% increase was detected 1 hour after exercise, indicating a short-term effect. In future studies it will be interesting to investigate whether the EIMD protocol can produce short-term responses in the muscles of the thigh, perhaps due to increased muscle perfusion following exercise.<sup>63</sup>

The values of  $|G^*|$  obtained predamage in this study were found to vary between 1–1.3 kPa over the thigh cross section which is in good agreement with Green et al,<sup>35</sup> who reported values for shear stiffness of 1 kPa. Other studies using similar techniques include Klatt et al,<sup>33</sup> and Barnhill et al,<sup>34</sup> who reported values for the storage modulus (i.e.,  $G'$ ) in the ranges of 0.7 to 2 kPa, and 1.0 to 1.9 kPa, respectively. These data, however, refer to a single frequency acquisition.  $G'$  values in the present study were derived from multifrequency data and ranged from 0.7 to 0.9 kPa. Multifrequency inversion will produce lower values due to the frequency dependence of the measurements and the contributions from acquisitions at frequencies lower than 50 Hz (i.e., 25 Hz and 37.5 Hz). This is the first study to measure  $\phi$  in muscle following exercise. The baseline values are in

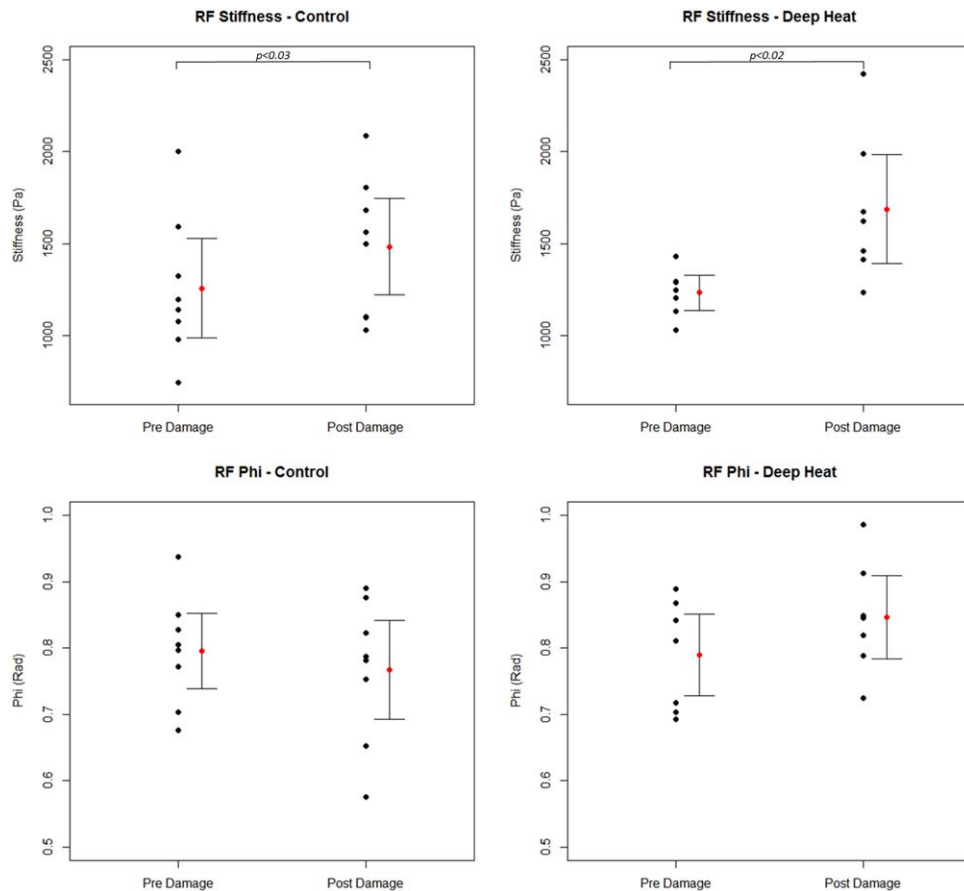


FIGURE 7: Values of  $|G^*|$  (upper row) and  $\varphi$  (lower row) in RF muscle for individual participants in the control (left column) and DH (right column) groups at baseline and 2 days after EIMD protocol.

good agreement with a previous study measuring  $\varphi$  of the quadriceps at rest.<sup>47</sup> Phase angle,  $\varphi$ , was found to decrease in the quadriceps in the DH group, with no significant change found in the control group. A reduction in  $\varphi$  may signify degradation of the structural matrix in the low-level tissue architecture,<sup>64</sup> perhaps indicating a greater destruction of actin and myosin cross-bridges due to strenuous exercise. This finding points to the DH group damaging more fibers during the EIMD protocol, a distinct possibility considering the significantly greater workload produced by the DH group. The lack of change in the RF, the site of most change in  $|G^*|$ , may be due to the small size of the RF muscle and hence the ROIs used, with scattering effects producing more heterogeneous results. These scattering effects are reduced in the  $|G^*|$  measurement due to the magnitude of both  $G'$  and  $G''$  being measured.

Several previous studies have investigated EIMD of the quadriceps muscle using techniques other than MRI. For example, Crenshaw et al<sup>65</sup> used a Biodex system to produce EIMD in eight healthy participants and showed that MVC was reduced by an average of 45%. Torres et al<sup>66</sup> also used a Biodex system to produce damage in the quadriceps muscle in 10 participants via eccentric contractions. The authors measured muscle stiffness using a Wartenberg pendulum

test, whereby increased muscle stiffness was identified by reduced range of motion and a slower angular velocity of the pendulum. Since the magnitude of the stiffness increase was similar to that found in the present study this suggests that the increased stiffness measured by Crenshaw et al<sup>65</sup> is directly related to changes in the muscle belly and not to contributions from tendons and ligaments.

The physiological mechanism underlying the muscle stiffness increase in EIMD has not been fully elucidated. Allen et al<sup>67</sup> postulated that the forcible lengthening of muscle fibers in EIMD leads to disruption at the level of the sarcomeres and which is exacerbated by repeated repetitions of the eccentric movement. This muscle fiber damage leads to release of  $\text{Ca}^{2+}$  into the cytoplasm in sufficient quantities that homeostasis is disturbed and contraction of fibers occurs. Swelling has also been cited as a potential reason for the increased passive stiffness.<sup>36–38</sup> However, Chleboun et al<sup>39</sup> have shown that, whereas stiffness may increase immediately following damage, swelling does not become significant until after 24 hours. In the present study participants in whom hyperintensity was observed on  $T_2$ -weighted images were found to show greater increase in muscle stiffness than participants who exhibited no increased  $T_2$  signal. This may be interpreted to suggest that an increase in fluid

volume associated with inflammation and edema produces increased muscle tension.

In future work we propose to use recent developments in MRE techniques including high SNR, high-resolution data acquisition sequences such as spiral MRE,<sup>68</sup> and state of the art super-resolution MRE based on data acquisition at multiple frequencies.<sup>47</sup> We will also incorporate diffusion tensor imaging (DTI) measurements of fiber orientation along with anisotropic inversion algorithms to correct for muscle fiber orientation.<sup>69</sup> Another consideration is whether the type of eccentric contraction has an effect on the distribution of damage within the muscle. For example, Takahashi et al<sup>70</sup> induced EIMD via an eccentric movement based on lowering the body down to a sitting position while balanced on one leg. Takahashi et al did not observe hyperintensity on  $T_2$ -weighted images of the RF following this eccentric movement; however, the VI, VM, and VL muscles did display hyperintensity. The movement utilized by Takahashi et al is a CKCE, and hence the vasti muscles are expected to be preferentially effected compared to the OKCE used in the present study.

There are several limitations of the study that should be discussed. First, the inversion step used in the analysis of MRE data assumes that the tissue is isotropic and homogeneous, but this is not strictly valid owing to the anisotropic orientation of the muscle fibers. Recent advances in MRE have led to the development of anisotropic inversion methods that utilize DTI to identify the primary fiber direction in the muscle and which has been incorporated into MRE data analysis.<sup>69</sup> A recent study has also employed a three-parameter inversion method to measure the anisotropic shear elastic parameters of skeletal muscle.<sup>71</sup> In addition, it should be noted that the EIMD protocol was designed to produce muscle damage regardless of the strength of the individual participants on account of a personalized workload having been set based on peak eccentric and concentric forces measured over three trials. However, if the participant did not fully engage with the experiment a sufficiently challenging workload may not be set and so the protocol may not produce EIMD. Each participant performed a familiarization session 48 hours prior to the EIMD protocol that aimed to reduce the former effects; however, perhaps further motivation and/or familiarization may be required for some participants. MRE data were only obtained on two occasions, at baseline and 48 hours after the EMD protocol, at which time muscle damage was suggested to peak.<sup>35</sup> Therefore, detailed knowledge of the time course of the stiffness response is limited. An interesting further development will be to obtain more detailed information on the changes in the mechanical properties of the muscle via pixel-by-pixel analysis of the MRE data for data obtained at intervals over a longer time period, and also to replace the qualitative assessment of signal intensity on  $T_2$ -weighted images with

computation of  $T_2$  relaxation time maps<sup>70</sup> coregistered with the elastograms.

In conclusion, we have demonstrated that MRE has the ability to detect skeletal muscle mechanical property changes in the quadriceps as a result of a personalized OKCE EIMD protocol. Complementary physiological and biochemical measurements enabled the confirmation of EIMD. DH participants were found to perform significantly more work during the EIMD protocol, yet recover MVC force faster. No significant difference in  $|G^*|$  was observed between groups; however,  $\varphi$  was significantly decreased in the quadriceps of the DH group. ROI analysis revealed that RF and VI muscles are preferentially affected by the eccentric contraction, with associated increased muscle stiffness and frequent  $T_2$  hyperintensity. Muscles displaying  $T_2$  hyperintensity were found to have an elevated stiffness change following damage compared to those which did not. The information obtained in this study suggests that DH rub may benefit participant force production during activity and facilitate accelerated return to normal activity after strenuous exercise. Further studies incorporating alternative exercise strategies are needed to determine if this outcome holds true following diverse exercise patterns.

## References

1. Howatson G, van Someren KA. The prevention and treatment of exercise-induced muscle damage. *Sports Med* 2008;38:483–503.
2. Warren GL, Lowe DA, Armstrong RB. Measurement tools used in the study of eccentric contraction-induced injury. *Sports Med* 1999;27:43–59.
3. Proske U, Morgan DL. Muscle damage from eccentric exercise: mechanism, mechanical signs, adaptation and clinical applications. *J Physiol* 2001;537:333–345.
4. Newham DJ, McPhail G, Mills KR, Edwards RHT. Ultrastructural changes after concentric and eccentric contractions of human muscle. *J Neurol Sci* 1983;61:109–122.
5. Nosaka K, Newton M. Difference in the magnitude of muscle damage between maximal and submaximal eccentric loading. *J Strength Cond Res* 2002;16:202–208.
6. Millet GY, Lepers R. Alterations of neuromuscular function after prolonged running, cycling and skiing exercises. *Sports Med* 2004;34:105–116.
7. Peake JM, Suzuki K, Wilson G, et al. Exercise-induced muscle damage, plasma cytokines, and markers of neutrophil activation. *Med Sci Sports Exerc* 2005;37:737–745.
8. Paddon-Jones DJ, Quigley BM. Effect of cryotherapy on muscle soreness and strength following eccentric exercise. *Int J Sports Med* 1997; 18:588–590.
9. Viitasalo JT, Niemelä K, Kaappola R, et al. Warm underwater water-jet massage improves recovery from intense physical exercise. *Eur J Appl Physiol* 1995;71:431–438.
10. Friden J, Sfikianos PN, Hargens AR. Muscle soreness and intramuscular fluid pressure: comparison between eccentric and concentric load. *J Appl Physiol* 1986;61:2175–2179.
11. Hunter AM, Galloway SD, Smith IJ, et al. Assessment of eccentric exercise-induced muscle damage of the elbow flexors by tensiomyography. *J Electromyogr Kinesiol* 2012;22:334–341.
12. Murayama M, Nosaka K, Yoneda T, Minamitani K. Changes in hardness of the human elbow flexor muscles after eccentric exercise. *Eur J Appl Physiol* 2000;82:361–367.

13. Shellock FG, Fukunaga T, Mink JH, Edgerton VR. Acute effects of exercise on MR imaging of skeletal muscle: concentric vs. eccentric actions. *Am J Roentgenol* 1991;156:765–768.
14. Skurvydas A, Kamandulis S, Stanislavaitis A, Streckis V, Mamkus G, Drazdauskas A. Leg immersion in warm water, stretch-shortening exercise, and exercise-induced muscle damage. *J Athl Train* 2008;43:592–599.
15. Rodenburg JB, Steenbeek D, Schiereck P, Bär PR. Warmup, stretching and massage diminish harmful effects of eccentric exercise. *Int J Sports Med* 1994;15:414–419.
16. Bixler B, Jones RL. High-school football injuries: effects of a post-halftime warmup and stretching routine. *Fam Pract Res J* 1992;12:131–139.
17. Wedderkopp N, Kalsoft M, Lundgaard B, Rosendahl M, Froberg K. Prevention of injuries in young female players in European team handball. A prospective intervention study. *Scand J Med Sci Sports* 1999;9:41–47.
18. Olsen O-E, Myklebust G, Engebretsen L, Holme I, Bahr R. Exercises to prevent lower limb injuries in youth sports: cluster randomised controlled trial. *BMJ* 2005;330:449.
19. McGowan CJ, Pyne DB, Thompson KG, Rattray B. Warm-up strategies for sport and exercise: mechanisms and applications. *Sports Med* 2015;45:1523–1546.
20. Lentell G, Hetherington T, Eagan J, Morgan M. The use of thermal agents to influence the effectiveness of a low-load prolonged stretch. *J Orthop Sports Phys Ther* 1992;16:200–207.
21. Henricson AS, Fredriksson K, Persson I, Pereira R, Rostedt Y, Westlin NE. The effect of heat and stretching on the range of hip motion\*. *J Orthop Sports Phys Ther* 1984;6:110–115.
22. Safran MR, Garrett WE, Seaber AV, Glisson RR, Ribbeck BM. The role of warmup in muscular injury prevention. *Am J Sports Med* 1988;16:123–129.
23. Strickler T, Malone T, Garrett WE. The effects of passive warming on muscle injury. *Am J Sports Med* 1990;18:141–145.
24. Noonan TJ, Best TM, Seaber AV, Garrett WE. Thermal effects on skeletal muscle tensile behavior. *Am J Sports Med* 1993;21:517–522.
25. Collins AJ, Notarianni LJ, Ring EF, Seed MP. Some observations on the pharmacology of “deep-heat”, a topical rubifacient. *Ann Rheum Dis* 1984;43:411–415.
26. Weingand K, Hengehold D, Knight E, et al. Topical heat provides pain relief of delayed onset muscle soreness of the distal quadriceps muscles. *Med Sci Sports Exerc* 1999;31.
27. Mason L, Moore RA, Edwards JE, McQuay HJ, Derry S, Wiffen PJ. Systematic review of efficacy of topical rubefacients containing salicylates for the treatment of acute and chronic pain. *BMJ* 2004;328:995.
28. Muthupillai R, Lomas D, Rossman P, Greenleaf J, Manduca A, Ehman R. Magnetic resonance elastography by direct visualization of propagating acoustic strain waves. *Science* 1995;269:1854–1857.
29. Hirata K, Miyamoto-Mikami E, Kanehisa H, Miyamoto N. Muscle-specific acute changes in passive stiffness of human triceps surae after stretching. *Eur J Appl Physiol* 2016;116:911–918.
30. McNair PJ, Stanley SN. Effect of passive stretching and jogging on the series elastic muscle stiffness and range of motion of the ankle joint. *Br J Sports Med* 1996;30:313–317.
31. Pišot R, Narici MV, Šimuniè B, et al. Whole muscle contractile parameters and thickness loss during 35-day bed rest. *Eur J Appl Physiol* 2008;104:409–414.
32. Dresner MA, Rose GH, Rossman PJ, Muthupillai R, Manduca A, Ehman RL. Magnetic resonance elastography of skeletal muscle. *J Magn Reson Imaging* 2001;13:269–276.
33. Klatt, Papazoglou S, Braun J, Sack I. Viscoelasticity-based MR elastography of skeletal muscle. *Phys Med Biol* 2010;55:6445–6459.
34. Barnhill E, Kennedy P, Hammer S, Beek EJR van, Brown C, Roberts N. Statistical mapping of the effect of knee extension on thigh muscle viscoelastic properties using magnetic resonance elastography. *Physiol Meas* 2013;34:1675.
35. Green MA, Sinkus R, Gandevia SC, Herbert RD, Bilston LE. Measuring changes in muscle stiffness after eccentric exercise using elastography. *NMR Biomed* 2012;25:852–858.
36. Howell JN, Chleboun G, Conatser R. Muscle stiffness, strength loss, swelling and soreness following exercise-induced injury in humans. *J Physiol* 1993;464:183–196.
37. Whitehead NP, Weerakkody NS, Gregory JE, Morgan DL, Proske U. Changes in passive tension of muscle in humans and animals after eccentric exercise. *J Physiol* 2001;533(Pt 2):593–604.
38. Howell JN, Chila AG, Ford G, David D, Gates T. An electromyographic study of elbow motion during postexercise muscle soreness. *J Appl Physiol* 1985;58:1713–1718.
39. Chleboun GS, Howell JN, Conatser RR, Giesey JJ. Relationship between muscle swelling and stiffness after eccentric exercise. *Med Sci Sports Exerc* 1998;30:529–535.
40. Stensdotter A-K, Hodges PW, Mellor R, Sundelin G, Häger-Ross C. Quadriceps activation in closed and in open kinetic chain exercise. *Med Sci Sports Exerc* 2003;35:2043–2047.
41. Escamilla RF, Fleisig GS, Zheng N, Barrentine SW, Wilk KE, Andrews JR. Biomechanics of the knee during closed kinetic chain and open kinetic chain exercises. *Med Sci Sports Exerc* 1998;30:556–569.
42. Paschalis V, Koutedakis Y, Baltzopoulos V, Mougios V, Jamurtas AZ, Giakas G. Short vs. long length of rectus femoris during eccentric exercise in relation to muscle damage in healthy males. *Clin Biomech Bristol Avon* 2005;20:617–622.
43. Delp SL, Loan JP. A graphics-based software system to develop and analyze models of musculoskeletal structures. *Comput Biol Med* 1995;25:21–34.
44. Knapik JJ, Wright JE, Mawdsley RH, Braun J. Isometric, isotonic, and isokinetic torque variations in four muscle groups through a range of joint motion. *Phys Ther* 1983;63:938–947.
45. Papazoglou S, Hamhaber U, Braun J, Sack I. Algebraic Helmholtz inversion in planar magnetic resonance elastography. *Phys Med Biol* 2008;53:3147–3158.
46. Barnhill E, Kennedy P, Johnson CL, Mada M, Roberts N. Real-time 4D phase unwrapping applied to magnetic resonance elastography. *Magn Reson Med* 2015;73:2321–2331.
47. Barnhill E, Hollis L, Sack I, et al. Nonlinear multiscale regularisation in MR elastography: Towards fine feature mapping. *Med Image Anal* 2016;35:133–145.
48. Klatt D, Hamhaber U, Asbach P, Braun J, Sack I. Noninvasive assessment of the rheological behavior of human organs using multifrequency MR elastography: a study of brain and liver viscoelasticity. *Phys Med Biol* 2007;52:7281–7294.
49. McGarry MDJ, Van Houten EEW, Perrinez PR, Pattison AJ, Weaver JB, Paulsen KD. An octahedral shear strain-based measure of SNR for 3D MR elastography. *Phys Med Biol* 2011;56:N153–164.
50. Yin Z, Glaser KJ, Manduca A, et al. Slip interface imaging predicts tumor-brain adhesion in vestibular Schwannomas. *Radiology* 2015;277:507–517.
51. Johnson CL, Holtrop JL, McGarry MD, et al. 3D multislab, multishot acquisition for fast, whole-brain MR elastography with high SNR efficiency. *Magn Reson Med* 2014;71:477–485.
52. Schneider CA, Rasband WS, Eliceiri KW. NIH Image to ImageJ: 25 years of image analysis. *Nat Methods* 2012;9:671–675.
53. Eston RG, Finney S, Baker S, Baltzopoulos V. Muscle tenderness and peak torque changes after downhill running following a prior bout of isokinetic eccentric exercise. *J Sports Sci* 1996;14:291–299.
54. Sayers SP, Clarkson PM. Force recovery after eccentric exercise in males and females. *Eur J Appl Physiol* 2001;84:122–126.
55. Honarvar M, Sahebjavaher R, Sinkus R, Rohling R, Salcudean SE. Curl-based finite element reconstruction of the shear modulus without assuming local homogeneity: time harmonic case. *IEEE Trans Med Imaging* 2013;32:2189–2199.

56. Baghani A, Salcudean S, Honarvar M, Sahebjavaher RS, Rohling R, Sinkus R. Travelling wave expansion: a model fitting approach to the inverse problem of elasticity reconstruction. *IEEE Trans Med Imaging* 2011;30:1555–1565.
57. Cournane S, Fagan AJ, Browne JE. Review of ultrasound elastography quality control and training test phantoms. *Ultrasound* 2012;20:16–23.
58. McAleavey S, Menon M, Elegbe E. Shear modulus imaging with spatially modulated ultrasound radiation force. *Ultrason Imaging* 2009;31:217–234.
59. Cohen J. *Statistical power analysis for the behavioral sciences*, 2nd ed. Hillsdale, NJ: Routledge; 1988.
60. Hather BM, Tesch PA, Buchanan P, Dudley GA. Influence of eccentric actions on skeletal muscle adaptations to resistance training. *Acta Physiol Scand* 1991;143:177–185.
61. Chen Y-W, Hubal MJ, Hoffman EP, Thompson PD, Clarkson PM. Molecular responses of human muscle to eccentric exercise. *J Appl Physiol* 2003;95:2485–2494.
62. Serrão FV, Foerster B, Spada S, et al. Functional changes of human quadriceps muscle injured by eccentric exercise. *Braz J Med Biol Res* 2003;36:781–786.
63. Selkow NM, Day C, Liu Z, Hart JM, Hertel J, Saliba SA. Microvascular perfusion and intramuscular temperature of the calf during cooling. *Med Sci Sports Exerc* 2012;44:850–856.
64. Hirsch S, Guo J, Reiter R, et al. MR elastography of the liver and the spleen using a piezoelectric driver, single-shot wave-field acquisition, and multifrequency dual parameter reconstruction. *Magn Reson Med* 2014;71:267–277.
65. Crenshaw AG, Thornell L-E, Fridén J. Intramuscular pressure, torque and swelling for the exercise-induced sore vastus lateralis muscle. *Acta Physiol Scand* 1994;152:265–277.
66. Torres R, Appell H-J, Duarte J. Acute effects of stretching on muscle stiffness after a bout of exhaustive eccentric exercise. *Int J Sports Med* 2007;28:590–594.
67. Allen DG, Whitehead NP, Yeung EW. Mechanisms of stretch-induced muscle damage in normal and dystrophic muscle: role of ionic changes. *J Physiol* 2005;567:723–735.
68. Johnson CL, McGarry MDJ, Van Houten EEW, et al. Magnetic resonance elastography of the brain using multi-shot spiral readouts with self-navigated motion correction. *Magn Reson Med* 2013;70:404–412.
69. Green MA, Geng G, Qin E, Sinkus R, Gandevia SC, Bilston LE. Measuring anisotropic muscle stiffness properties using elastography. *NMR Biomed* 2013;26:1387–1394.
70. Takahashi H, Kuno S, Miyamoto T, et al. Changes in magnetic resonance images in human skeletal muscle after eccentric exercise. *Eur J Appl Physiol* 1994;69:408–413.
71. Guo J, Hirsch S, Scheel M, Braun J, Sack I. Three-parameter shear wave inversion in MR elastography of incompressible transverse isotropic media: Application to in vivo lower leg muscles. *Magn Reson Med* 2016;75:1537–1545.